ELSEVIER

Journal of Photochemistry and Photobiology A: Chemistry 142 (2001) 187–195

Journal of Photochemistry and Photobiology A:Chemistry

www.elsevier.com/locate/jphotochem

Anomalies in the linear absorption, transient absorption, photoluminescence and photoluminescence excitation spectroscopies of colloidal InP quantum dots

Garry Rumbles*, Donald C. Selmarten, Randy J. Ellingson, Jeffrey L. Blackburn, Pingrong Yu, Barton B. Smith, Olga I. Mićić, Arthur J. Nozik

Center for Basic Sciences, National Renewable Energy Laboratory, Golden, CO 80401, USA

Abstract

We report photoluminescence (PL), linear absorption and femtosecond, transient bleaching spectra for a colloidal solution of indium phosphide (InP) quantum dots (QDs) at ambient temperature. The PL quantum yield is shown to depend significantly upon the excitation wavelength and the PL excitation spectrum deviates markedly from the absorption spectrum. The cooling of electrons and holes to the lowest energy excited state is determined, by transient bleaching spectroscopy, to occur with an efficiency that is independent of the excitation wavelength.

These results are discussed in terms of a threshold for a non-radiative decay process that resides above the bandgap and a PL quantum yield that depends upon the size of QD.

Keywords: Linear absorption; Transient absorption; InP quantum dots; Photoluminescence

1. Introduction

The electronic spectroscopy of colloidal semi-conductors affords an ideal opportunity to investigate the properties of quantum confined systems and to explore how these systems deviate from their bulk counterparts. The bulk of studies on colloidal quantum dots (QDs) are focused on the II–IV class of materials and specifically cadmium selenide [1,2]. The main attention for III–V materials has focused on indium phosphide (InP) [3,4] and indium arsenide (InAs) [5]. Both classes exhibit similar quantum confinement properties, exhibiting a shift in the bandedge of the electronic absorption spectrum to higher energy when the diameter of the quantum dot drops below ca. 80 Å. To confer solubility on the QDs and create colloidal solutions, organic surfactant ligands are bound to the surface of the QD. These are typically trioctylphosphine oxide (TOPO) or trioctylphosphine (TOP), both of which are also critical in the controlled-growth synthesis in solution of the QDs. These ligands also help to reduce the impact of uncoordinated surface bonds, which, in a species where 30% of the constituent atoms can reside at the surface are a major influence on the excited state photophysics. Photoluminescence (PL) studies of these systems has verified the importance of terminating the surface in a controlled fashion, in order that surface states do not act as quenching sites for the confined excitons and extinguish the luminescence. The use of a high-energy bandgap material, such as zinc sulphide [6], has proven successful in this regard for CdSe. While a controlled etch with ultra-dilute hydrogen fluoride of InP QDs has proven equally successful in yielding QDs that exhibit significant PL quantum yields [8].

The electronic absorption spectra of QDs in solution are characterized by a distinct excitonic peak on the low energy, bandedge side of the spectrum followed by an increase in the absorption coefficient at higher energies [9,10]. The synthesis of these systems is non-trivial and even after careful purification procedures, the samples can still exhibit a finite distribution in size of 10% or even higher. In circumstances where the size distribution has been reduced significantly, the spectrum reveals more distinct features [1]. The lowest energy transitions for QDs have been successfully identified from a number of theoretical perspectives and agree well with experimental observations [11–14]. The electronic absorption features are considered sharp and atomic-like and the main broadening mechanism for the absorption spectrum is considered to be inhomogeneous broadening due to the finite size distribution. InP, for example, exhibits absorption transitions with a linewidth of 5 meV at 20 K, and is predicted to rise to 60 meV at ambient temperatures [15]. The lowest energy absorption feature can be 250 meV wide, however. Photoexcitation of a QD with a photon of high energy yields an initial state with both unthermalized electrons

* Corresponding author

1010-6030/01/$ – see front matter
PII: S1010-6030(01)00513-5

and holes. The high effective mass of the holes in the valence band combined with the closely spaced energy levels results in efficient thermalization to the top of the band. The effective mass of the electron in the conduction band is lower, however, and this can lead together with the attendant more widely-spaced energy levels to a less efficient cooling mechanism. This process, known as the phonon bottleneck, has been the subject of a number of recent investigations, which have shown the importance of electron-hole interactions via an Auger-like process to cool the electron down to the bottom of the conduction band [7,16,18–21]. Thus, like their molecular counterparts, QDs are generally expected to follow Kasha's rule [22] with the emission emanating from the lowest excited state in the QD. The global emission from a QD sample is also broadened, therefore, by its finite size distribution. An implication of an efficient relaxation of both electrons and holes is that the PL excitation spectrum of an optically thin sample will closely resemble the absorption spectrum. For CdSe, however, there is evidence that these two spectra differ at high energies [12,23] and that there exists a threshold for a non-radiative decay mechanism [23].

Preliminary studies on InP reveal a similar phenomenon that may point towards the phonon bottle neck as the mechanism responsible for this effect [24]. In this article, we report further studies on dilute solutions of colloidal InP in hexane, studied using a number of spectroscopies that are sensitive to the energetics of the photoexcited electrons and holes. The objective is to elucidate the origin of the discrepancy between absorption and PL excitation spectra for colloidal QDs.

2. Experimental

Colloidal nanocrystalline InP was synthesized, purified and characterized according to the procedure published previously [3]. Hexane (Aldrich) was tested for extraneous luminescence and was used without further purification. Solutions that also contained excess TOPO were purged with helium to remove dissolved oxygen and transferred to 1 cm pathlength, fused silica cuvettes for absorption and emission measurements. Electronic absorption spectra were recorded using a double beam spectrometer (Cary 500) at a spectral resolution of 1 nm. The PL emission and excitation (PLE) spectra were recorded using a spectrometer with a photon-counting detection system and a 450 W xenon discharge lamp as an excitation source (Fluorolog 2). Spectral resolution for both PL and PLE was fixed at 1 nm using two additive dispersion double monochromators (1.8 nm/mm dispersion). All emission and excitation spectra were corrected for the wavelength dependence of the detection and excitation systems, respectively. Transient bleaching data were recorded with excitation from a visible OPO pumped by the output of an amplified, mode-locked Ti:Sapphire laser (Clark CPA 2001); a system that provides wavelength tunable, 125 fs pulses at a repetition rate of 1 kHz. White light (440–950 nm) pulses were generated by focussing the 775 nm output of the pump laser into a 2 mm-thick sapphire plate: compensation for the spectral chirp provided a temporal resolution <200 fs. Transient bleach spectra were measured on solutions contained in 2 mm pathlength cells by recording the white light spectrum with and without alternate pump laser pulses.

3. Results

The electronic absorption data for etched and unetched InP QD samples in hexane at 295 K are shown in Fig. 1. The lowest energy absorption peak, or exciton peak, occurs at ca. 630 nm and is indicative of a dot diameter of 38 ± 4 Å

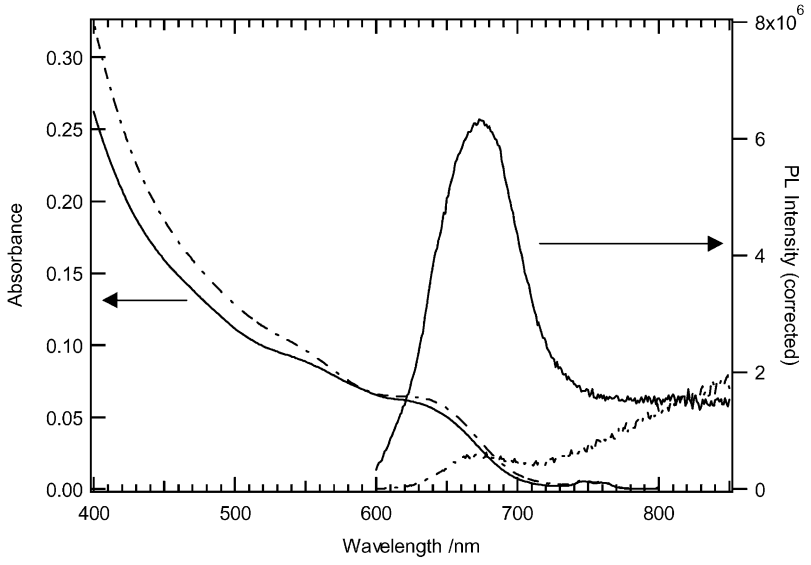

Fig. 1. Absorption and emission spectra ($\lambda_{ex} = 640$ nm) for dilute solutions of unetched (dashed line) and etched colloidal quantum dots of InP in hexane.

[9,13]. The slight spectral blue shift of the etched sample with respect to the unetched sample is attributed to a modest reduction in the average dot size due to the etching process [8]. The shoulder at 550 nm corresponds to a transition to the second excited state. Although detailed energy level diagrams are available for InP QDs and predict a number of energy states in the region of these two broad spectral features [14], we refer to these here as transitions to the 1S and 1P states.

The PL spectra for the two samples exciting at 640 nm are also shown in Fig. 1. The effect of etching can be seen to increase the emission at 675 nm by an order of magnitude, while the deep red emission at 850 nm decreases marginally.

The PL spectra, corrected for the sensitivity of the detection system, of the etched sample as a function of excitation wavelength are shown in Fig. 2a for excitation wavelengths at 20 nm intervals ranging from 420 to 660 nm. These data are plotted against energy, for accurate determination of the PLQY at each excitation wavelength, and the intensity reflects counts per second per energy bandwidth [25]. The data are offset for clarity and the sharp peak on the high energy side of each spectrum is due to scattered excitation light. Fig. 2b displays data for excitation at 400 and 660 nm with corresponding fits to a Gaussian and Lorentzian lineshape function.

Two PL excitation spectra (PLE) for the etched sample were recorded by detecting (i) wavelength-integrated emission and (ii) emission at a fixed wavelength of 675 nm, which corresponds to the peak of the global emission. These data are shown in Fig. 3 and they have been corrected for the wavelength-dependent response of the Si photodetector used to monitor the intensity of the excitation lamp. A %

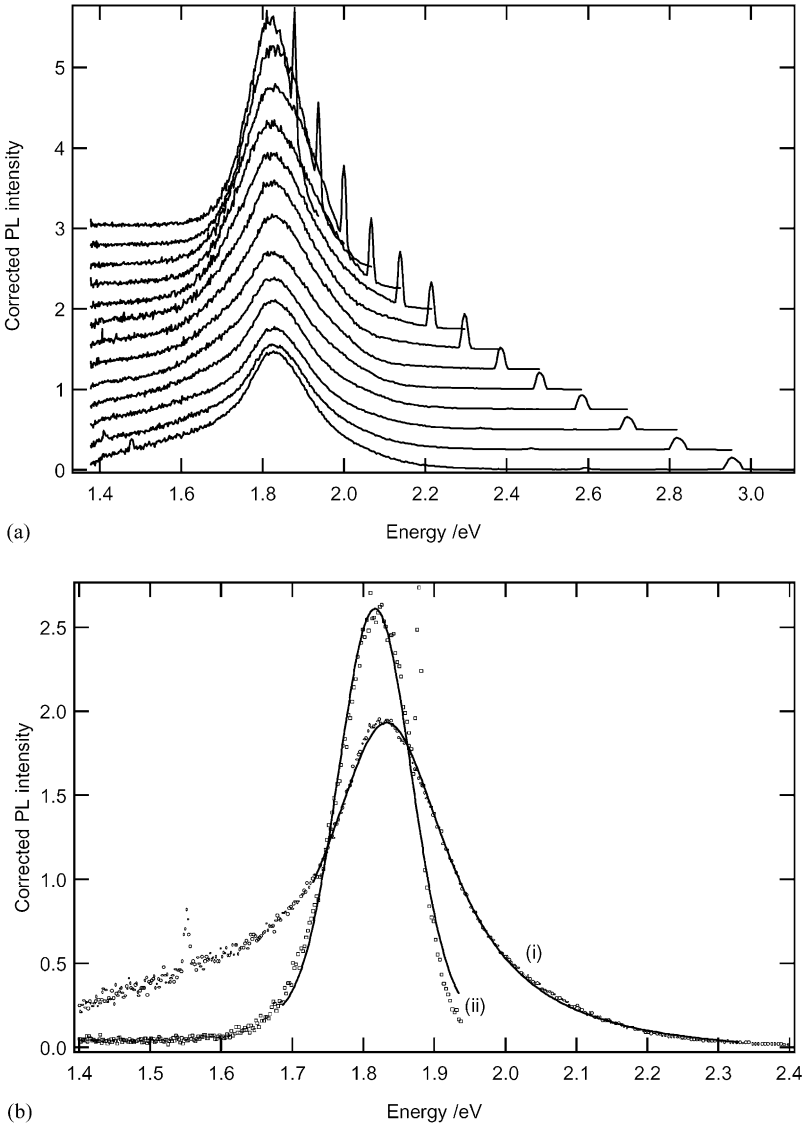

Fig. 2. (a) Corrected photoluminescence emission spectra exciting at 20 nm intervals from 420 to 660 nm. The sharp peaks at high energy are scattered excitation light. (b) Comparison of spectra exciting at 400 and 660 nm with fits (solid line) to a Lorentzian and a Gaussian function, respectively.

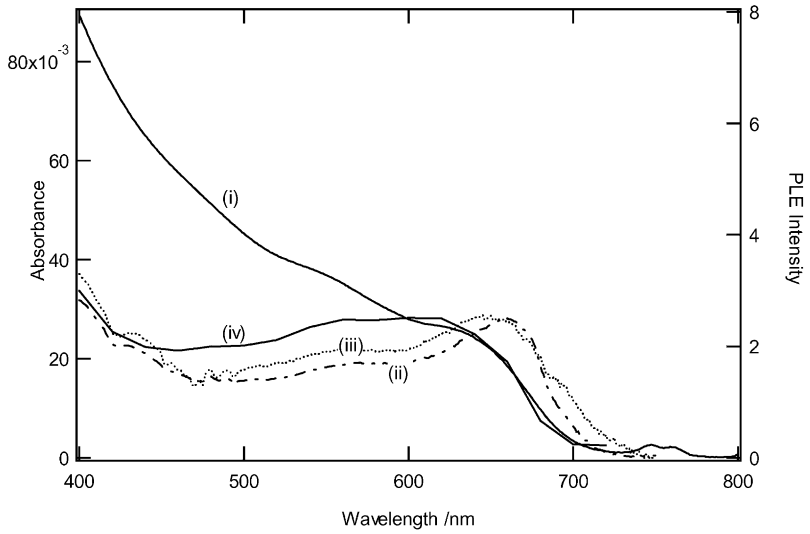

Fig. 3. Comparison of (i) %absorption, and photoluminescence excitation spectra measured detecting; (ii) emission at 675 nm; (iii) integrated emission and (iv) integrated area beneath spectra in Fig. 2.

absorption (%*A*) spectrum, derived from Fig. 1, that corresponds to the effective absorption at the center of the 1 cm cuvette, is also shown in the figure, along with the relative PLQY values derived from the data shown in Fig. 2.

Transient bleach spectra for the etched sample are shown in Fig. 4, with excitation at 461, 511 and 625 nm and at a time delay of 50 ps. The pump power was adjusted to ensure that the excitation density was kept to approximately 0.4 excitations per dot, using a procedure reported elsewhere [7]. There is little difference between these spectra, with the strong signal at 630 nm corresponding to the bleach signal of the 1S transition, and the small peak at 530 nm attributed to the 1P transition.

4. Discussion

The effects of etching the InP QD sample are consistent with previous published results [8], with the sharp exciton emission growing significantly in magnitude while the deep trap emission at longer wavelengths is reduced, but to a lesser extent.

The effects of the excitation wavelength on the emission profile are evident in Fig. 2. For excitation in the range 2.95 eV (420 nm) to 2.07 eV (600 nm), the emission profile remains broad, with a bandwidth of 213 meV. For lower energy excitation the width reduces to 120 meV at 1.88 eV (660 nm) and 100 meV at 1.77 eV (700 nm), an effect that

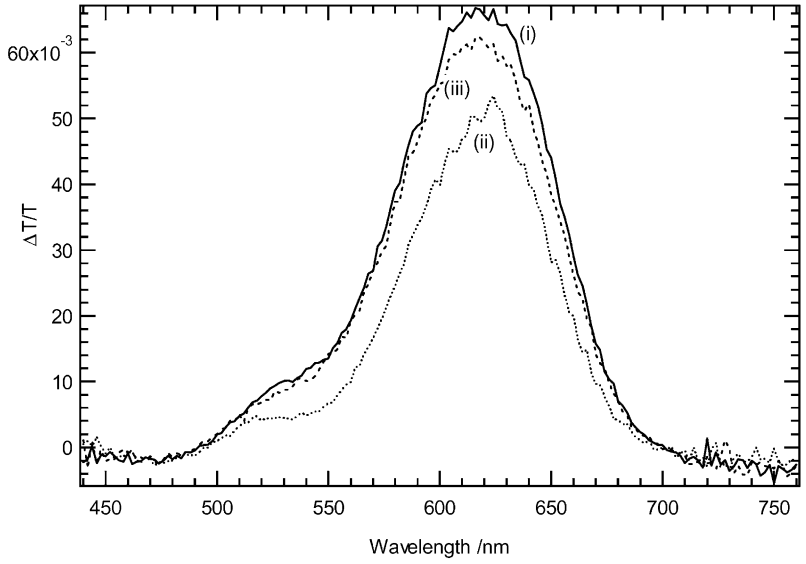

Fig. 4. Transient bleach spectra recorded after 50 ps with excitation at (i) 461 nm; (ii) 511 nm and (iii) 625 nm.

can be seen more clearly in Fig. 2b. Luminescence line narrowing has been demonstrated and explained before [9,14,26–28] and is attributed to excitation of the larger dots within the finite size distribution that absorb preferentially on the low energy side of the absorption profile. This, however, does not explain why the emission spectrum sharpens on the low energy side as well. A plausible explanation could be less efficient deep trap emission from the larger QDs too. Interestingly, for excitation at 3.1 eV (400 nm) the emission spectrum can be described very well by a Lorentzian lineshape, as shown in Fig. 2b, while the data for excitation at 660 nm is modeled more closely by a Gaussian function. The applicability of a Lorentzian function is an unexpected observation, and a full rationalization cannot be given at this stage. This may be fortuitous with the emission on the high-energy side of the peak originating from a separate transition that lies beneath the main transition. The fact that both the Lorentzian lineshape and the low energy emission disappear as the excitation energy is reduced may mean that there is another separate, broad emission that lies beneath the main exciton emission peak. Note that the peak intensity of the PL with excitation at 1.88 eV is greater than that observed for excitation at 3.1 eV, even though the absorbance at this higher energy is nearly five times as great.

This observation is more apparent when the PLE spectra are compared to the absorption data shown in Fig. 3. As discussed earlier, the PLE spectra are a measure of $\%A$, which approximates to the absorbance for samples of low optical density. The geometry deployed in the PLE experiments uses a 1 cm cuvette with emission detected perpendicular to excitation. To avoid inner filter effects, the optical density of the sample must be kept <0.1, where $\%A$ and absorbance are very similar. From Fig. 1, the absorbance at wavelengths shorter than 500 nm rises to 0.25 at 400 nm. The $\%A$ spectrum depicted in Fig. 3 compensates for this effect, and is determined from

$$\%A \propto [10^{-0.4\mathrm{OD}} - 10^{-0.6\mathrm{OD}}] \quad (1)$$

Where OD is the absorbance of the solution in the 1 cm cuvette, as shown in Fig. 1, and $\%A$ is determined for the central 2 mm of the sample cuvette, from which the emission is detected. Such a procedure thus eliminates any errors that may arise for the absorption of the excitation light at the shorter wavelengths. The resultant spectrum, shown in Fig. 3, is very similar to that in Fig. 1, which indicates that the inner filter effect is only a minor one. The PLE data exhibit the same phenomenon as noted for the PL data of Fig. 2, with short excitation wavelengths yielding less PL than those around the bandedge. The peak of the PLE spectrum depends upon type of emission detected. For wavelength-integrated emission, the PLE spectrum peaks at 650 nm, while detecting emission at a fixed wavelength of 675 nm it peaks at a slightly longer wavelength of 660 nm. Of these two wavelengths, neither coincide with the absorption maximum or the peak of the transient bleach signal, shown in Fig. 4. It appears from these spectra that the PL from the larger dots is more intense, a result that is in agreement with the intensities of the two PL spectra shown in Fig. 2b. The surface of a QD plays a major role in the nonradiative decay of the excited state, thus, the lower surface to volume ratio of the smaller QDs may be expected to exhibit more nonradiative decay and, hence, less emission. The PLE data shown in Fig. 3 are not ideal however. By detecting emission at 675 nm, the PLE spectrum is biased towards those QDs that emit at this wavelength; a form of size-selective spectroscopy. The detection of wavelength-integrated emission should obviate this problem and this could explain why the peak of this PLE spectrum is shifted 10 nm to the blue, compared to detecting emission at 675 nm. However, this method does not compensate for the wavelength sensitivity of the detection system. By integrating the areas beneath the corrected PL spectra, shown in Fig. 2a, a more accurate determination of the PLE spectrum can be derived, and this is also shown in Fig. 3. Using this approach, the PLE spectrum does coincide well with the low-energy absorption feature but, like the other two PLE spectra, it deviates markedly at higher energies. These data suggest that not all the excitation energy at these higher energies results in emission from the bandedge of the dot. This could be due to a non-radiative decay channel that is accessible only at high excitation energies, or that the solution is inhomogeneous and contains species that absorb and do not emit.

The solutions are optically translucent and there is no direct evidence of aggregation, which would increase particle sizes and enhance the scattering cross-section. Thus, the possibility that the large optical density at short wavelengths is due to scattering can be excluded. TOPO, used in excess to ensure that the QDs remain in solution, exhibits only a weak absorbance at wavelengths shorter than 400 nm, and this too can be excluded as the origin of the high optical density. The absorbance at high energies may be attributed to small QDs that emit less efficiently than their larger counterparts and with a spectrum that is markedly broader. This could in fact be the origin of the broad spectrum that lies beneath the main spectral feature, shown in Fig. 2, and proposed earlier as the origin of the apparent Lorentzian lineshape. This interpretation suggests that the PLE spectrum is actually a good measure of the absorption spectrum for a narrow distribution of large QDs. This idea does not agree well with previous experiments or theory, both of which suggest that the absorbance in the high energy region is greater than at the bandedge due to a greater number of overlapping transitions in this spectral region.

Alternatively, the effect may be due to a non-radiative decay route for the excited state, accessible only by excitation at short wavelengths. The efficiency of relaxation to the emitting state would, therefore, not be 100%, and would depend upon the excess energy of the exciting photon above that of the bandgap. A similar conclusion has been drawn for CdSe QDs dispersed in a polymer matrix, where the PLQY was

shown dependent on the excitation wavelength [23]. These authors concluded that there existed a threshold above the bandgap, where a continuum of states acts as a sink for the excitation energy. It is unclear what the origin of this continuum of states represents, but a similar threshold is also evident in InP QDs.

The theory of the phonon bottleneck [16,18,29,30], where the transition from the 1P state to the emitting, 1S, state is hindered by requirement of multiphonon-electron scattering events, may offer a possible explanation of the threshold. While the PLE spectrum and absorption spectrum agree reasonably well at the bandedge, a significant deviation does occur at 550 nm, the position of the 1P transition. If the 1P state acts as a longer-lived trap state, then it may be more susceptible to non-radiative decay and, hence, lead to less bandedge emission. This explanation would also be applicable to the case of CdSe.

In order to investigate this possibility further, femtosecond transient absorption spectroscopy was used to study the relaxation of the excited state, in a fashion that has been used successfully for CdSe QDs. This is achieved by following the spectroscopy and kinetics of the bleaching signals corresponding to the 1S and 1P transitions. The transient bleach spectra, shown in Fig. 4, were recorded for three different excitation, or pump, wavelengths: 625, 511 and 461 nm, at a time delay of 50 ps following excitation. These wavelengths correspond to excitation of the 1S, 1P and an undefined high-energy state, respectively. All three spectra peak at the same wavelength of 620 nm, which coincides well with the bandedge of the linear absorption spectrum in Fig. 1. The small feature at 530 nm is attributed to residual bleaching of the transition to the 1P state. These data were recorded with a pump power adjusted to ensure that the number of excited QDs was the same at the three pump wavelengths. If all excited states relaxed with 100% (or the same) efficiency to the bandedge, then the magnitude of the transient bleach signals would be expected to be almost the same, and within experimental error this appears to be the case.

Thus, this observation contrasts with the prediction of a high-energy, non-radiative decay channel, described earlier, which would predict a smaller signal for the bleach signal when pumping at 461 nm than at 625 nm. The phonon bottleneck model would also predict that the bleach signal for the 1P state would be long lived, as the energy became trapped in this state. The transient bleach kinetics for the 1S and 1P states are shown in Fig. 5 for the same three pump wavelengths of 461, 511 and 625 nm. The origin of the bleach signal at early times is a combination of both state filling and carrier induced Stark effect [7]. This must be taken into consideration when explaining these data, although the emphasis here is on state filling. The bleach signals of the 1S transition, measured at 616 nm (Fig. 5a) are very similar in absolute magnitude, with an initial $\Delta\alpha/\alpha = -0.14 \pm 0.02$ an initial relaxation time constant of approximately 20 ps that extends to 170 ps at longer times. Close inspection of the rise-time of these data (not shown) reveals a slower time constants for excitation at 461 and 511 nm, consistent with relaxation of the initially excited state back down to the 1S state. The kinetic data for the relaxation of the 1P state, measured at 525 nm, are shown in Fig. 5b and show marked differences with excitation wavelength. For excitation at 625 nm the excitation energy is insufficient to promote an electron to the 1P state and, therefore, the bleach signal can be tentatively be attributed to the hole thermalized at the top of the valence band. The effective mass ratio of holes to electrons in InP QDs is >10 [17], which means that the holes relax to a thermalized state at the top of the valence band far more efficiently than the electrons to the bottom of the conduction band [19]. The difference in the bleach signals of the 1P state, when pumping at 461 and 511 nm, can therefore be attributed to the electrons. At early times the bleach signal is large ($\Delta\alpha/\alpha = -0.03 \pm 0.01$) and decays with a time constant of approximately 1 ps. At longer times, this extends to a value of ca. 30 ps, similar to that for excitation at 625 nm, and to the 20 ps time constant for the initial relaxation of the 1S state. The fast, 1 ps kinetics of the 1P state may be attributed to the efficient relaxation of the 1P state to the 1S state, although these values do not coincide well with the risetimes of the 1S state. However, the importance of the carrier-induced Stark effect may also complicate the data recorded at very early times. The transient bleach data of the 1P state suggest that the electron does exist in the 1P state for longer than 300 ps. This observation seems to confirm the idea of a bottleneck in the relaxation process, but the excess thermal energy of the electron should be transferred to the hole via an Auger process [20]. After 300 ps, however, the transient spectrum remains almost identical to that recorded after 50 ps (Fig. 4). This might be attributed to efficient hole trapping at the surface of our InP QDs, which would inhibit electron cooling by an Auger process [20]. The peak of the global PL occurs at 1.84 eV and the transient bleach signal at 1.98 eV, thus, a considerable relaxation in energy occurs between the two states responsible for these two signals. This may be caused by a splitting of the lowest energy hole state by electron-hole exchange, as now proposed for CdSe QDs [31].

The shortest component of the PL decay is 28 ns and the longest component almost 200 ns [9]. The PL emission data reported here are all steady-state and are therefore integrated over even longer time-scales than this. The difference between these data and the sub-nanosecond transient bleach data reported here, must be taken into consideration when examining the differences between the two experiments. A non-radiative decay process that can compete with relaxation of the electrons and holes to the 1S state would occur on a fast time-scale and would have been detectable in our transient bleaching experiments. Thus, although the two experiments span different time regimes, the idea that a non-radiative decay channel at high energies can explain the loss of PL, seems inconsistent.

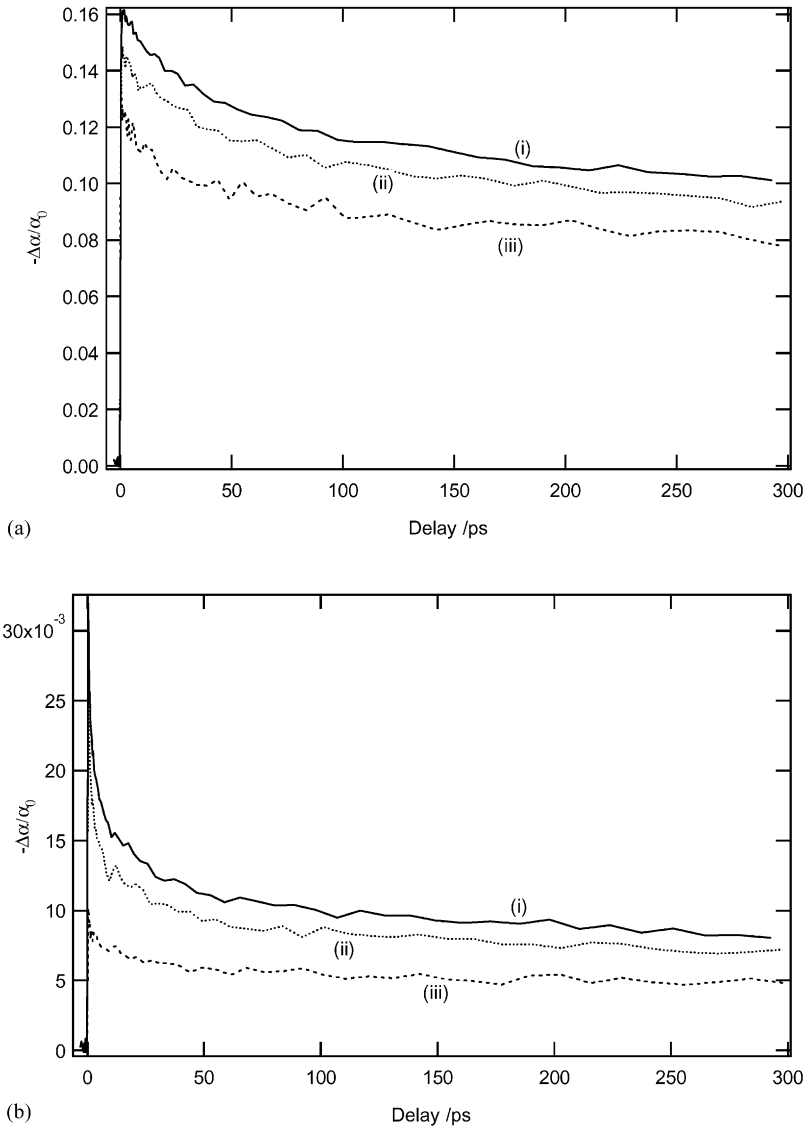

Fig. 5. Transient bleaching signals with excitation at (i) 461 nm; (ii) 511 nm and (iii) 625 nm. Signal detected for (a) the 1S transition at 616 nm and (b) the 1P transition at 525 nm.

In summary, the transient bleaching data reveals the number of electron-pairs that reach the lowest 1S state is independent of the excitation wavelength, while the PL data indicate that the number reaching the emissive state does depend upon the excitation wavelength. If the discrepancy between the two experiments is attributed to the differing time-scales, then the emissive state must retain a memory of the initial excitation wavelength. To reflect the excess energy of excitation, one possibility is the excess energy remains as thermal energy within the QD. Using a heat capacity of $0.322\,\mathrm{JK^{-1}\,g^{-1}}$ and a 30 Å diameter QD the QD temperature would rise by only 8 K, which is too small to invoke a more efficient non-radiative decay.

A more plausible explanation is the absorption at high energies by small QDs that emit with lower quantum efficiency than the larger QDs. The relaxation to the 1S state would be similar for all QDs and excitation wavelengths and, hence, the magnitude of the transient bleach data would correlate well with the linear absorption coefficient, but the PL would reflect only the larger QDs. Importantly, this result also rules out the possibility that the absorption is due to an impurity species. The difference observed for the two PL spectra in Fig. 2b could thus be attributed to a sharper emission peak from the larger QDs, with an underlying broader emission from the smaller QDs in the sample. The combination of these two spectra would yield a spectrum that has a fortuitous Lorentzian lineshape profile. Based on this interpretation the PLE spectra shown in Fig. 3 would represent the true absorption spectrum of the larger QDs in our sample, with the measured absorption spectrum representing a broader distribution of QDs than

first thought. Although this argument is consistent with our data, it still contrasts with theoretical expectations of a rising absorption coefficient at short wavelengths due to a greater density of states. Also, previous independent studies of the distribution of QD sizes using TEM do not reveal the presence of the large fraction of small QDs that are implicated here [32]. On the other hand, the higher energy absorption coefficients for small QDs would be high, due to its inverse cubic dependence on QD diameter, and therefore, the contribution to the overall absorption spectrum would be enhanced.

5. Conclusion

The PL spectra of a solution of colloidal quantum dots of InP show a marked dependence upon the excitation wavelength, with the PL intensity at short wavelengths being far less than would be predicted from the amount of absorption. Although this observation might be explained by a threshold for non-radiative decay above the bandgap [23], or even evidence for a phonon bottleneck [29,30], transient bleaching data do not concur. The number of electron-hole pairs that relax back to the emitting 1S state are in direct proportion to the amount of absorbed light, regardless of the excitation wavelength as determined by the magnitude of the bleaching signal for the 1S state.

An interpretation that is consistent with the results from both experiments is a PL quantum yield that depends upon the size of the QD. Large QDs emit efficiently at 675 nm, while small QDs, that are absorbing preferentially at short wavelengths, emit with a broad emission spectrum that lies beneath the 675 nm peak. Although the analysis is consistent with data reported here, they are in contrast to previous work. Specifically, the size distribution of a QD a sample determined by TEM shows a narrow, Gaussian-shaped size-distribution with few, if any, very small QDs, but the sample still exhibits an absorption spectrum similar to that reported here [32]. In addition, the PLE spectra are indicative of the large, emissive QDs and yet they still do not show an increase in the absorption coefficient at high energies, as predicted by theory. There is some evidence for trapping of electrons in the 1P state up to 300 ps after excitation, which does lend credibility to the theory of a bottleneck in the relaxation process. The possibility that the high-energy emission, assigned at present to small QDs, emanates from the 1P state has been considered, but this again does not explain the bleaching recovery data for the 1S state.

Regardless of the model used to explain the data, it is clear that the interpretation of the measured absorption spectrum requires further investigation, as the origin of the absorbance at high energy and the fate of the resulting excitation are not known unequivocally. Colloidal QDs offer many opportunities for applications that range from biological labels to electro-optic devices. In most cases, this requires exploitation of the broad absorption spectrum and narrow emisison, and consequences of the uncertainties reported here must therefore be known.

Acknowledgements

We would like to thank the US Department of Energy, Office of Science, Office of Basic Energy Sciences, Division of Chemical Sciences for generous financial support. Garry Rumbles would like to thank the Center for Basic Science, NREL and the Department of Chemistry, Imperial College for support as a sabbatical research scientist.

References

[1] C.B. Murray, C.R. Kagan, M.G. Bawendi, Ann. Rev. Mater. Sci. 30 (2000) 545.
[2] C.B. Murray, D.J. Norris, M.G. Bawendi, J. Am. Chem. Soc. 115 (1993) 8706.
[3] O.I. Mićić, J. Sprague, C.J. Curtis, K.M. Jones, J.L. Machol, A.J. Nozik, H. Geissen, B. Fluegel, G. Mohs, N. Peyghambaian, J. Phys. Chem. 99 (1995) 7754.
[4] A.A. Guzelian, J.E.B. Katari, A.V. Kadavanich, U. Banin, K. Hamad, E. Juban, A.P. Alivisatos, R.H. Wolters, C.C. Arnold, J.R. Heath, J. Phys. Chem. 100 (1996) 7212.
[5] A.A. Guzelian, U. Banin, A.V. Kadavanich, X. Peng, A.P. Alivisatos, Appl. Phys. Lett. 69 (1996) 1432.
[6] M. Danek, K.F. Jensen, C.B. Murray, M.G. Bawendi, Chem. Mater. 8 (1996) 173.
[7] V.I. Klimov, J. Phys. Chem. B. 104 (2000) 6112.
[8] O.I. Mićić, J. Sprague, Z. Lu, A.J. Nozik, Appl. Phys. Lett. 68 (1996) 3150.
[9] O.I. Mićić, H.M. Cheong, H. Fu, A. Zunger, J.R. Sprague, A. Mascarenhas, A.J. Nozik, J. Phys Chem. B 101 (1997) 4904.
[10] D.J. Norris, M.G. Bawendi, Phys. Rev. B. 53 (1996) 16338.
[11] A.I. Ekimov, F. Hache, M.C. Schanne-Klein, D. Ricard, C. Flyzanis, I.A. Kudryavtsev, T.V. Yazeva, A.V. Rodina, Al.L. Efros, J. Opt. Soc. Am. 10 (1993) 100.
[12] D.J. Norris, Al.L. Efros, M. Rosen, M.G. Bawendi, Phys. Rev. B. 53 (1996) 16347.
[13] H. Fu, A. Zunger, Phys. Rev. B. 56 (1997) 1496.
[14] H. Fu, A. Zunger, Phys. Rev. B. 57 (1998) R15064.
[15] U. Banin, G. Cerullo, A.A. Guzelian, C.J. Bardeen, A.P. Alivisatos, C.V. Shank, Phys. Rev. B. 55 (1997) 7059.
[16] A.J. Nozik, Ann. Rev. Phys. Chem. 52 (2001) 193.
[17] S. Wang, Fundamentals of Semiconductor Theory and Device Physics, Prentice-Hall, Englewood Cliffs, 1989, p. 523.
[18] H. Benisty, C.M. Sotomayor-Torrs, C. Weisbuch, Phys. Rev. B. 44 (1991) 10945.
[19] V.I. Klimov, Ch.J. Schwartz, D.W. McBranch, C.A. Leatherdale, M.G. Bawendi, Phys. Rev. B. 60 (1999) R2177.
[20] V.I. Klimov, A.A. Mikhailovsky, D.W. McBranch, C.A. Leatherdale, M.G. Bawendi, Science 287 (2000) 1011.
[21] V.I. Klimov, A.A. Mikhailovsky, D.W. McBranch, C.A. Leatherdale, M.G. Bawendi, Phys. Rev. B. 61 (2000) R13349.
[22] M. Kasha, Rad. Res. Suppl. 2 (1960) 243.
[23] W. Hoheisel, V.L. Colvin, C.S. Johnson, A.P. Alivisatos, J. Chem. Phys. 101 (1994) 8455.
[24] G. Rumbles, D.C. Selmarten, R.J. Ellingson, J.L. Blackburn, P. Yu, B.B. Smith, O.I. Mićić, A.J. Nozik, Proc. Mat. Res. Soc. Symp. Proc., in press.
[25] J.R. Lakowicz, Principles of Fluorescence Spectroscopy, 2nd Edition, Kluwer Academic Publishers, Dordrecht, 1999, p. 52.

[26] U. Banin, A. Mews, A.V. Kadavanich, A.A. Guzelian, A.P. Alivisatos, Mol. Cryst. Liq. Cryst. A 283 (1996) 1.
[27] M. Nirmal, C.B. Murray, M.G. Bawendi, Phys. Rev. B. 50 (1994) 2293.
[28] D.J. Norris, M. Nirmal, C.B. Murray, A. Sucra, M.G. Bawendi, Z. Phys. D 26 (1993) 355.
[29] U. Brockelmann, Phys. Rev. B 48 (1993) 17637.
[30] H. Bensity, Phys. Rev. B 51 (1995) 13281.
[31] V.I. Klimov, A.A. Mikhailovsky, S. Xu, A. Malko, J.A. Hollingsworth, C.A. Leatherdale, H.-J. Eisler, M.G. Bawendi, Science 290 (2000) 314.
[32] A.J. Nozik, O.I. Mićić, MRS Bull. 23 (1998) 24.